The
CRISPR
Journal

RESEARCH ARTICLE

Single-Step, High-Efficiency CRISPR-Cas9 Genome Editing in Primary Human Disease-Derived Fibroblasts

Matteo Martufi,[1] Robert B. Good,[2] Radu Rapiteanu,[1] Tobias Schmidt,[1] Eleni Patili,[1] Ketil Tvermosegaard,[1] Maria New,[1] Carmel B. Nanthakumar,[2] Joanna Betts,[1] Andy D. Blanchard,[2] and Klio Maratou[1],*

Abstract

Genome editing is a tool that has many applications, including the validation of potential drug targets. However, performing genome editing in low-passage primary human cells with the greatest physiological relevance is notoriously difficult. High editing efficiency is desired because it enables gene knockouts (KO) to be generated in bulk cellular populations and circumvents the problem of having to generate clonal cell isolates. Here, we describe a single-step workflow enabling >90% KO generation in primary human lung fibroblasts via CRISPR ribonucleoprotein delivery in the absence of antibiotic selection or clonal expansion. As proof of concept, we edited two SMAD family members and demonstrated that in response to transforming growth factor beta, SMAD3, but not SMAD2, is critical for deposition of type I collagen in the fibrotic response. The optimization of this workflow can be readily transferred to other primary cell types.

Introduction

One of the remaining challenges for genome editing is to perform experiments in primary cells isolated from patient or healthy donor tissues and used experimentally at low passages to minimize cell changes in culture. The most widely used workflows for genome editing involve monoclonal cell isolation prior to subsequent characterization of the effect of the edit. The generation of clonal cells ensures that phenotypic experiments are performed using a uniform, genetically identical population of cells. However, primary cells cannot proliferate indefinitely or survive outside of specific culture conditions, and therefore are not amenable to monoclonal selection or clonal expansion following genome editing. One solution is to use the pool of edited cells (bulk cell culture) directly for experimental analysis. In this case, the editing efficiency needs to be sufficiently high, so that so that a large proportion if not all cells contain the desired modification at all copies of the target locus. Such analysis is suited for functional analysis of genes and pathways, as it accelerates the timelines for validation of novel targets and leads to a better understanding of the biological mechanisms underlying human diseases.

To develop genome editing workflows in human primary cells, we chose to focus on primary human lung fibroblasts, which are important for the study of molecular pathways involved in idiopathic pulmonary fibrosis (IPF). Patients with IPF have a poor prognosis, with median survival of 3 years post diagnosis, and a progressive loss of lung function due to the synthesis and deposition of a local, dense, collagen-rich extracellular matrix (ECM).[1] Understanding the mechanisms underpinning ECM secretion and deposition has important therapeutic implications, and therapeutic approaches targeting these mechanisms are being explored clinically. The ability to knock out individual genes rapidly and effectively in freshly isolated cells from patients would provide a valuable early target validation platform to assess novel mechanistic approaches.

Accurate genotyping of the edited cells is an important requirement for bulk cell culture editing pipelines. It confirms on-target editing and provides precise measurements of the editing events. Most commonly, genotyping is achieved by Surveyor nuclease,[2] T7 endonuclease I (T7E1) assay,[3] TIDE assay,[4] or droplet digital polymerase chain reaction (PCR).[5] These methods are low throughput,

[1]Target Sciences and [2]Fibrosis Discovery Performance Unit, Respiratory Therapy Area, Medicines Research Centre, GlaxoSmithKline R&D, Stevenage, United Kingdom.

*Address correspondence to: Klio Maratou, Target Sciences, Medicines Research Centre, GlaxoSmithKline R&D, Gunnels Wood Road, Stevenage, SG1 2NY, Stevenage, United Kingdom, E-mail: klio.x.maratou@gsk.com

cannot be easily multiplexed, and do not provide accurate sequence information on the achieved edits. Moreover, they can't be easily used to genotype a bulk population of cells with several different mutations. The development of workflows that use targeted deep sequencing[6–10] has solved this problem and paved the way for automated, target-focused genome editing at scale. Our lab adopted the publicly available sequence-evaluation tool Out-Knocker,[6,7] which allows rapid identification of all-allelic frameshift mutations in bulk cellular populations.

Here, we describe how we established a CRISPR-Cas9 ribonucleoprotein (RNP) complex workflow to carry out highly efficient genome editing in a bulk population of primary fibroblasts derived from IPF patients without applying any selection. To optimize the electroporation of RNP complex delivery into fibroblasts, we edited gene *PI4KA* and established conditions enabling full gene knockout (KO) in bulk cells with a single round of electroporation. Using these conditions, we could replicate results with multiple targets, and we present SMAD2 and SMAD3 single KOs, as well as a double KO, as a proof of concept. The pipeline described in this paper is presented as a tool that can be applied in target validation studies for drug discovery in allowing the rapid and efficient genomic modification of any gene and further opens the possibility to identify associated clinical biomarkers.

Methods

Study approval

Samples of IPF lung tissue were obtained from patients undergoing lung transplant or surgical lung biopsy following informed signed consent and with research ethics committee approval (11/NE/0291, 10/H0504/9, 10/H0720/12, and 12/EM/0058). Lung tissues were obtained from Newcastle Upon Tyne Hospitals NHS Foundation Trust. Blood was obtained from Clinical Trials Laboratory Services. The human biological samples were sourced ethically, and their research use was in accordance with the terms of the informed consents under an IRB/EC approved protocol. All experiments were performed in accordance with relevant guidelines and regulations.

Cell culture of primary human lung fibroblasts

Primary human lung fibroblasts were grown from explant culture of IPF lung tissue, as described previously.[11] Cells were cultured in Dulbecco's modified Eagle's medium (DMEM; #21969; Gibco) supplemented with 10% heat-inactivated fetal bovine serum (FBS) and Glutamax. Cells were kept in a humidified 10% CO_2 atmosphere at 37°C. Fibroblast vials were thawed at passage 2 and electroporated with CRISPR-Cas9 RNP complex 2 days after.

Cell culture of primary human CD4+ T cells

Primary human CD4+ T cells were prepared by obtaining peripheral blood mononuclear cells from human blood using Leucosep tubes (#227288; Greiner), followed by depletion of CD8+ cells with Miltenyi MACS (130-097-196, 130-093-545), expansion of the remaining T-cell population by stimulation with Transact (130-109-104; Miltenyi), and freezing of expanded cells. Vials were thawed at passage 2 and electroporated with CRISPR-Cas9 RNP complex 3–5 days after. Cells were cultured in RPMI 1640 (31870-025; Invitrogen) supplemented with 10% heat-inactivated FBS and Glutamax and 10 ng/mL of interleukin 7 (premium grade; cat. no. 130-095-362; Miltenyi). Cells were kept in a humidified 10% CO_2 atmosphere at 37°C.

CRISPR-Cas9 RNP electroporation in primary human lung fibroblast

SMAD2, *SMAD3*, and *PI4KA* crRNA design was achieved using the free online tool Deskgen. The crRNA sequences are reported in Supplementary Table S1. Alt-R crRNAs and Alt-R tracrRNA were acquired from IDT and resuspended in nuclease-free duplex buffer (IDT) at a concentration of 100 μM. One microliter from each of the two RNA components was mixed together and diluted in nuclease-free duplex buffer at a concentration of 25 μM. The mix was boiled at 95°C for 5 min and cooled at room temperature for 10 min. The annealed RNA (2.9 μL), corresponding to 72.5 pmol, was complexed with 60 pmol of Cas9 to a ratio of 1.2:1, unless stated otherwise. The mix was left at room temperature for 10 min. Afterwards, 60 pmol of electroporator enhancer (IDT) was added and incubated at room temperature with the RNP complex for 5 min.

Passage 2 cells from IPF donors were electroporated when around 80% confluent. A detailed electroporation protocol can be found in the Supplementary Data. For the 4D Nucleofector System (Lonza) experiments, 250,000 cells in 20 μL were used per electroporation. Cells were washed once in phosphate-buffered saline (PBS), and pelleted by centrifugation at 90g, 10 min, at room temperature. After PBS removal, cells were re-suspended in 15.5 μL of P3 solution from a P3 Primary Cell 4D-Nucleofector® X Kit (Lonza) and mixed together with 4.5 μL of RNP complex to reach a total volume of 20 μL. Electroporation was performed in 16-well Nucleocuvette™ strips using program CM-138. For a double KO generation using the 4D Nucleofector system, RNPs targeting SMAD2 exon 6 and SMAD3 exon 6 were complexed *in vitro* as described above. A total of 250,000 cells were washed once in PBS, and pelleted by centrifugation at 90g, 10 min, at room temperature.

After PBS removal, cells were re-suspended in 11 μL of P3 solution and mixed together with 9 μL of RNPs to reach a final volume of 20 μL. Electroporation was performed in 16-well Nucleocuvette™ Strips using program CM-138.

For the 2b Nucleofector System (Lonza) experiments, 1,000,000 cells in 100 μL were used alongside a Basic Nucleofector™ Kit for Primary Mammalian Fibroblasts (Lonza). After PBS removal, cells were re-suspended in 90 μL of Basic Nucleofector™ Solution for Mammalian Fibroblasts.

CRISPR-Cas9 RNP electroporation in primary CD4^{+} T cells

Alt-R crRNA and Alt-R tracrRNA were re-suspended in nuclease-free duplex buffer at a concentration of 100 μM. Six microliters (270 pmol) of each RNA component was mixed, boiled at 95°C, and cooled at room temperature for 10 min to make 540 pmol of annealed RNA. This was then complexed with 180 pmol of Cas9 (at a ratio of 1:3) for 10 min at room temperature. Expanded CD4+ T cells ($n = 1,000,000$) derived from peripheral blood were re-suspended in 20 μL of P3 primary Cell 4D-Nucleofector X Kit Buffer (Lonza) and were then mixed with 15 μL of RNP complex for a total of 35 μL. Electroporation was carried out using a 4D Nucleofector system in 16-well Nucleocuvette Strips™ with the EH-115 program. Protein knockdown efficiency of major histocompatibility complex Class I in CD4+ primary T cells was measured via flow cytometry. Cells were stained with the PE antihuman HLA ABC antibody (#311405; Biolegend) followed by acquisition on a CytoFLEX X flow cytometer (Beckman Coulter). Quantification was then performed using FlowJo v10.

MiSeq genotyping analysis

Genotyping was carried out, as described by Schmid-Burgk et al.[6] All PCR primers are illustrated in Supplementary Tables S2 and S3. Briefly, 24 h after electroporation, 10,000 cells were collected and re-suspended in 10 μL of lysis buffer (0.2 mg/mL of proteinase K, 1 mM of CaCl$_2$, 3 mM of MgCl$_2$, 1 mM of EDTA, 1% Triton X-100, 10 mM of Tris, pH 7.5). Cells were incubated for 10 min at 65°C and 15 min at 95°C to generate a cell lysate, and 2 μL of lysate was added in a first PCR reaction to amplify the genomic locus that flanks the CRISPR target site. A second PCR, using 1 μL of the first PCR product, attaches Illumina adaptor and barcode sequence for sequencing and later deconvolution. For all PCRs, Phusion® High-Fidelity Master Mix with HF Buffer (Thermo Fisher Scientific) and an annealing temperature of 63°C were

used. After the second PCR, samples were pooled and purified using AMPure XP beads (Beckman Coulter Life Sciences) in a beads/PCR product ratio of 0.8:1. After purification, the sequencing library was quantified using a NanoDrop™ instrument (Thermo Fisher Scientific). Five nanograms of library was denatured and diluted for next-generation sequencing using a MiSeq instrument (Illumina) following the manufacturer's instructions. Libraries were clustered and sequenced using 300 bp single-end sequencing with a MiSeq Reagent Kit v2 (MS-102-2002; Illumina). Sequencing reads were analyzed using the online tool OutKnocker v1.31 using default parameters, as described by Schmid-Burgk et al.[6]

Scar-in-a-Jar

After genome editing, fibroblasts were left in culture for 1 week. Cells were then plated in a 96-well clear imaging microplates (BD Falcon) at a concentration of 1×10^4 cells/well in DMEM (0.4% FBS). After 24 h, cells were incubated in modified medium containing 0.4% of FBS, 16.7 μg/mL of ascorbic acid, 37.5 mg/mL of Ficoll 70, and 25 mg/mL of Ficoll 400 to generate macromolecular crowding conditions. Transforming growth factor beta (TGF-β; 1 ng/mL) was also added, and fibroblasts were left at 37°C for 72 h before being fixed in ice-cold methanol and permeabilized in 0.1% Triton-X-100 in PBS. Immunostaining was performed by overnight incubation at 4°C with anti-collagen type I antibody (C2456; Sigma–Aldrich) at 1:1,000 dilution in PBS. Cells were then incubated for 1 h at room temperature with secondary antibody Alexa Fluor 488 goat anti-mouse immunoglobulin G (IgG; A11001; Invitrogen) at 1:500 dilution and Hoeschst dye (H3570; Invitrogen) at 1:10,000 dilution in PBS. A further staining step with anti-αSMA antibody (C6198; Sigma–Aldrich) at 1:1,000 dilution in PBS was carried out for 1 h at room temperature. The culture plate was scanned using a CellInsight NXT HCS instrument (Thermo Fisher Scientific) at $10\times$ magnification.

Scar-in-a-Jar results and statistical analysis

Statistical analyses were performed in R. A linear mixed effects model was fitted to the data using a fixed-effect term corresponding to interaction between genotype (SMAD2 KO, SMAD3 KO, or wild type), TGF-β (plus or minus), and donor (1 or 2). A random effect of date was included to account for day-to-day variations in the overall response level. The fit was performed using the R package lme4.[12] The model described above was fitted separately to log2 of the collagen response and log2 of the αSMA response. Because the interaction of genotype and TGF-β with donor was statistically significant in both

fits, the effect of KO within TGF-β-stimulated cells was examined on a donor-by-donor basis using estimated marginal means obtained via the R package emmeans. To ease data visualization in Figure 4E, the estimated contrasts (KO-wild type, within TGF-β-stimulated cells, for KO = SMAD2 KO and SMAD3 KO) and their confidence intervals were back-transformed from the log2 scale.

Western blot

Protein extracts were produced using a cell pellet washed twice with PBS. Cells ($n = 500,000$) were lysed in $50\,\mu\text{L}$ of RIPA buffer and left at 4°C for 30 min. The lysate was spun at $16,800\,\text{g}$ for 15 min, and $20\,\mu\text{L}$ of supernatant was recovered and run on a 4–20% sodium dodecyl sulfate polyacrylamide gel. Proteins were transferred onto a polyvinylidene fluoride membrane using the iBLOT system (Invitrogen) for 6 min using program P3. The membrane was incubated with anti-SMAD 2/3 antibody (#8685; Cell Signaling Technology) at 1:1,000 dilution or anti-Actin antibody (A2228; Sigma–Aldrich) as a loading control at 1:2,000 dilution at 4°C overnight. Secondary goat anti-rabbit IgG HRP antibody (A16096; Invitrogen) was used at 1:2,000 dilution for the anti-SMAD2/3 detections, while secondary rabbit anti-mouse IgG HRP antibody (A16160; Invitrogen) was used at 1:5,000 dilution with anti-actin. Both secondary antibodies were incubated for 1 h at room temperature. Visualization of membranes was performed using the machine Syngene G:BOX with the software Genesnap.

Data availability

All data generated or analyzed during this study are included in this published article (and its Supplementary Data).

Results

Optimization of workflow for genome editing in primary human lung fibroblasts

We hypothesized that phenotypic assays could be performed in bulk populations with >90% of alleles for a gene of interest containing indel mutations, since this would translate into a very low chance of obtaining a cell carrying two wild-type alleles. To achieve this, we based our experiments on RNP delivery using electroporation. We built our workflow using the commercially available Alt-R CRISPR-Cas9 system (IDT), which is comprised of a chemically modified crisprRNA (crRNA) and trans-activating crisprRNA (tracrRNA) complexed with Cas9 protein.

To fine-tune our workflow, we focused on generating KO cells for phosphatidylinositol 4-kinase alpha (PI4KA),

a moderately expressed cell signaling protein. A critical factor in successful gene editing is the choice of highly efficient crRNAs. We first carried out screening of eight crRNAs targeting different exons of *PI4KA* in order to identify the two best performing ones (Supplementary Fig. S1). The RNP complex was delivered by electroporation using a Nucleofector 2b device with manufacturer recommended electroporation conditions (Supplementary Fig. S1). Primary fibroblasts were left in culture for 24 h before being collected and genotyped through targeted deep sequencing using an Illumina MiSeq system.[7] Analysis of the generated mutations was carried out with the freely available Web tool Out-Knocker,[6] which provides detailed information on the type and frequency of mutations in the allele population (Fig. 1, stage 1). Despite screening for multiple crRNAs, we observed that editing efficiency was too low to enable functional analysis of the bulk cellular population (Supplementary Fig. S1). Therefore, we complemented the crRNA selection with a thorough optimization of the electroporation delivery step.

We made a side-by-side comparison of the Lonza Nucleofector 2b and 4D systems. For the 2b system, we utilized a Basic Nucleofector kit for Primary Fibroblasts and the already established and manufacturer recommended program A-24. However, this could not be transferred to the 4D system, and therefore we proceeded with testing several electroporation programs via transfecting cells with the positive control plasmid pmaxGFP, which is included in each Nucleofector™ Kit (Supplementary Fig. S2A), and the P3 Primary Cell 4D-Nucleofector™ X Kit. Three electroporation programs (CA137, CM137, and CM138) were selected on the basis of transfection efficiency and cell morphology. To find the best program, an RNP complex, formed using 15 pmol of Cas9 with a RNA/Cas9 ratio of 1.2:1, was delivered to the cells targeting exon 1 of the *B2M* gene, which has previously been successfully used in other cell types[13,14] (Supplementary Fig. S2B). Alongside optimization of the electroporation program, we tested the benefits of co-transfection with the Alt-R Cas9 electroporation enhancer (IDT). Inclusion of the enhancer dramatically increased indel generation (Supplementary Fig. S2B). Genome editing efficiency was similar among the three programs. However, we decided to use the Nucleofector 4D program CM138 due to better cell recovery after electroporation. With the B2M guide, we only achieved approximately 45% editing efficiency. However, for this target, we used a guide optimized for other cell types where high efficiency was not required. To proceed with final optimizations, we returned to use of the *PI4KA* exon 10 guide RNA selected after the initial
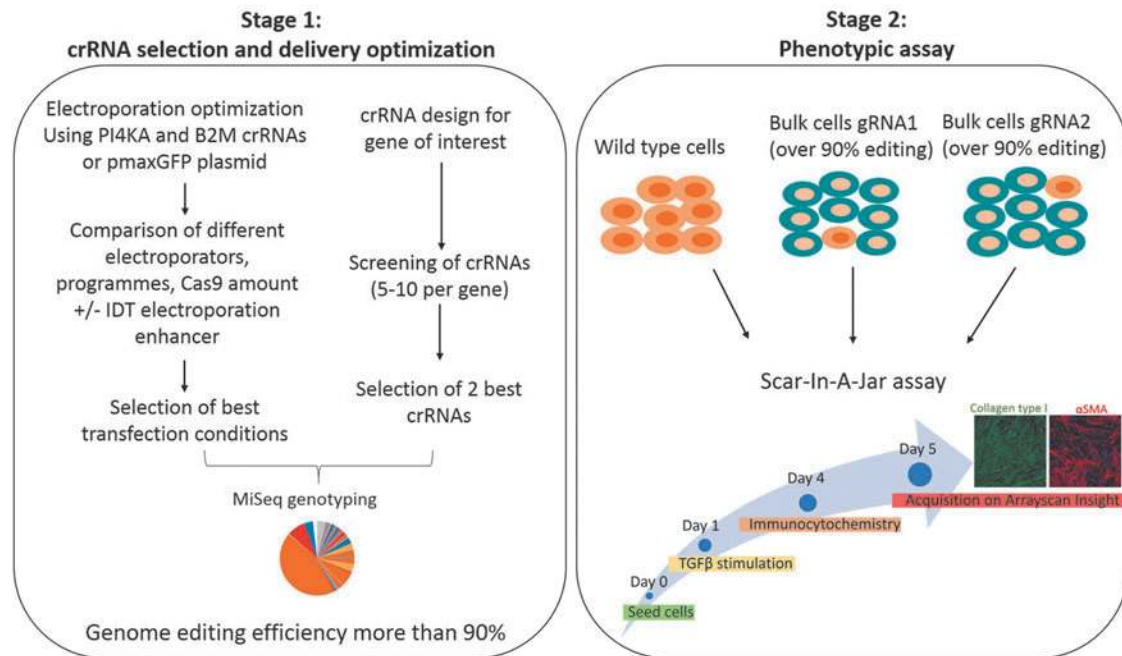
FIG. 1. Pipeline of genome editing in primary human lung fibroblasts. Stage 1: Parameters such as different Nucleofector systems, electroporation programs, Cas9 amounts, electroporation buffers, and an electroporation enhancer were tested to find the best condition in terms of cell morphology, cell viability, and genome editing efficiency. gRNA screening of 5–10 per gene was carried out to select the two best gRNAs. Genotyping of the bulk cell population to quantify the editing efficiency was performed by MiSeq sequencing and OutKnocker analysis. The pie chart represents alleles in the cell population, with distinct colors for wild-type sequences, in-frame indels, or out-of-frame indels. Stage 2: Bulk cell populations with >90% indels were used to perform the Scar-in-a-Jar phenotypic assay. This assay measures type I collagen deposition and the with nct colors for wtransforming growth factor beta (TGF-β) stimulation.

guide RNA screening described above (Supplementary Fig. S1). This time, we increased the amount of Cas9 to 60 pmol per reaction. For Nucleofector 2b, we could not achieve very high editing efficiency with only one electroporation, and therefore we had to perform another round of electroporation to reach indel frequencies that would allow us to perform phenotypic assays in a bulk population. Contrarily, for Nucleofector 4D, a single-round of electroporation in the presence of the electroporation enhancer using program CM138 with 60 pmol of Cas9 with a RNA/Cas9 ratio of 1.2:1 was enough to achieve 100% editing efficiency (Fig. 2B). This condition was used to perform all remaining experiments described in this paper.

SMAD3 KO affects the fibrotic response to TGF-β stimulation

Once cells have been edited with high efficiency, they can be assayed within a disease-relevant phenotypic assay. We tested for collagen type I deposition and

alpha smooth-muscle actin (αSMA) expression driven by TGF-β stimulation and macromolecular crowding using a high-content imaging assay termed Scar-in-a-Jar (Fig. 1, stage 2).[15,16] This phenotypic, high-content screening method quantifies the amount of extracellular collagen deposition to deliver a robust and reliable endpoint to study the effect of gene ablation in fibrosis.

To demonstrate the utility of our workflow in a setting relevant to fibrosis, we knocked out two closely related proteins critical to TGF-β signaling (SMAD2 and SMAD3). These are two transcription factors involved in the activation of the fibrotic response and are responsible for the upregulation of genes such as collagen type I and αSMA.[17] Seven gRNAs targeting different exons were tested for each gene (sequence shown in Supplementary Table S1). The exon 6 *SMAD3* gRNA, showing nearly 100% mutation efficiency, alongside the exon 6 *SMAD2* gRNA, exhibiting nearly 80% mutation efficiency, were selected for progression to phenotypic experiments using the Scar-in-a-Jar assay (Fig. 3A). The
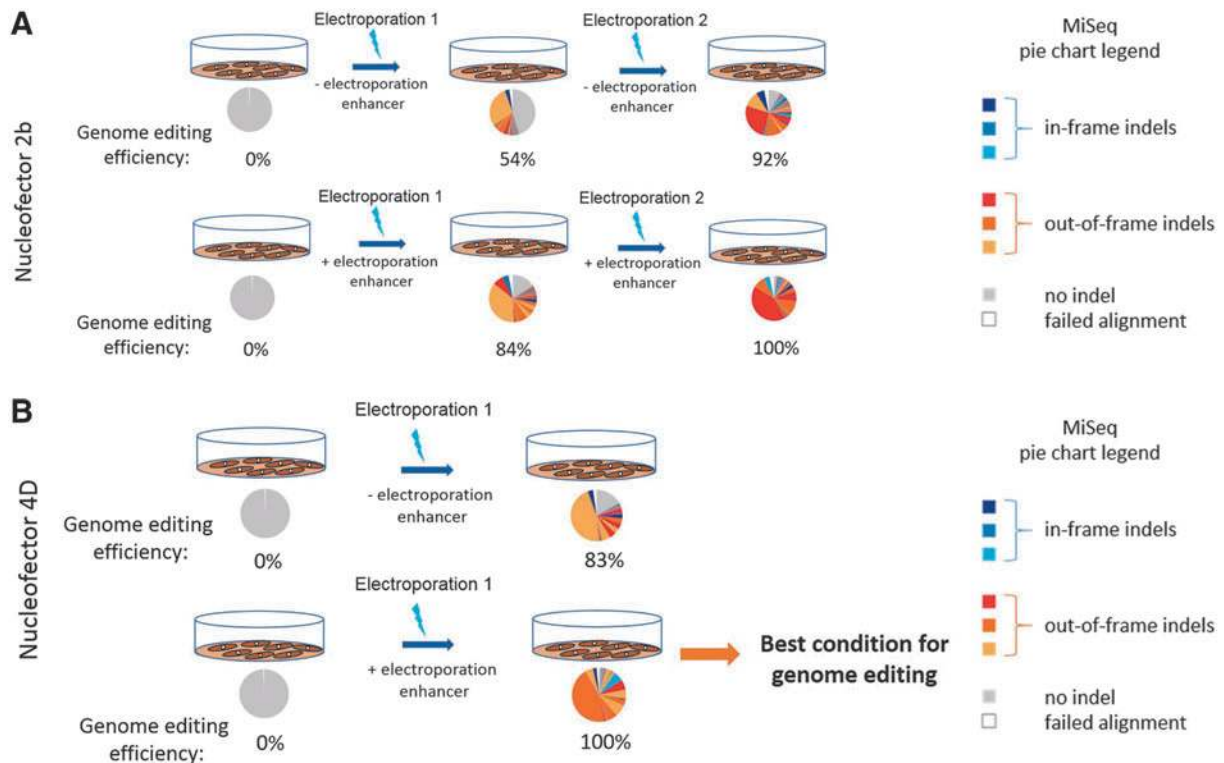
FIG. 2. Phosphatidylinositol 4-kinase alpha (*PI4KA*) genome editing optimization. Comparison between the Nucleofector 2b and the 4D was carried out by using a gRNA targeting exon 10 of *PI4KA*, and experiments were performed in the presence and absence of an electroporation enhancer. Cells were collected 24 h after electroporation and genotyped by MiSeq and OutKnocker Web tool analysis. The pie chart represents the OutKnocker analysis output. Every pie chart represents a cellular pool, while colors of the individual pie areas indicate in-frame mutations (blue), out-of-frame mutations (red), or no indel calls (gray). **(A)** For Nucleofector 2b, two rounds of electroporation were required to achieve high genome editing efficiency, even in the presence of an electroporation enhancer. **(B)** For Nucleofector 4D, one round of electroporation was sufficient for high editing efficiency.

exon 6 *SMAD2* gRNA performed with around 94% editing efficiency when the experiment was subsequently repeated (Fig. 3B; donor 1 cells *n* = 4, donor 2 cells *n* = 3). The *SMAD3* exon 2, exon 4, and exon 6 guides also showed consistently high editing efficiencies with experimental repeats (Fig. 3B), providing us with high confidence in our workflow. The high efficiency in generating mutations in the two gene loci is mirrored by absence of the proteins. Although SMAD2 and SMAD3 proteins share >90% of protein sequence homology, Western blot analysis confirmed that each KO was protein specific (Fig. 4A).

In a separate experiment, a double KO of both proteins in the same cell population was performed. We chose the exon6 gRNAs for both *SMAD2* and *SMAD3* and co-delivered the RNP complexes during the same electroporation. The experiment was performed in cells derived from two donors. Genotyping of both loci showed highly

efficient genome editing for both genes in the same sample (Supplementary Fig. S3). This was confirmed by Western blot that showed ablation of both proteins (Fig. 4A).

Using the exon 6 gRNAs targeting *SMAD3* and *SMAD2*, we performed Scar-in-a-Jar assays in cells derived from two different donors (*n* = 3 for donor 1; *n* = 2 for donor 2). KO of SMAD3 resulted in a dramatic reduction in collagen deposition in comparison to the wild-type IPF fibroblasts, while KO of SMAD2 did not show any reduction (Fig. 4B and C and Supplementary Fig. S4). We checked the levels of αSMA as an additional phenotypic measurement. This gene is upregulated when fibroblasts undergo myofibroblast differentiation after TGF-β stimulation and is a crucial requirement to enable cells to produce collagen.[18] The SMAD3 KO cells lacked αSMA expression, while the SMAD2 KOs showed increased expression in comparison to wild-type cells (Fig. 4B and C
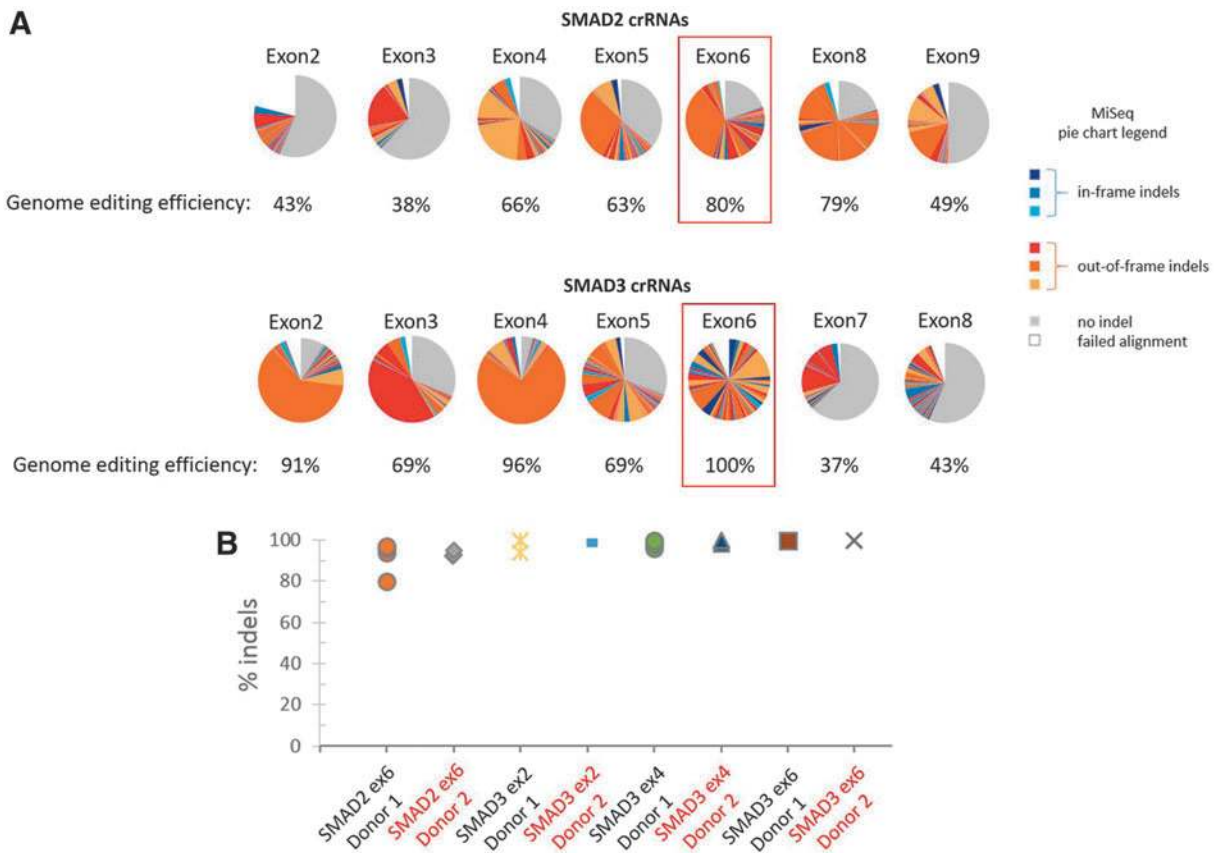
FIG. 3. Efficient genome editing for *SMAD2* and *SMAD3*. **(A)** Pie charts represent the OutKnocker genotyping analysis results from one representative experiment, and illustrate the mutations generated by gRNAs targeting different exons for *SMAD2* and *SMAD3*. The crRNAs highlighted were chosen to edit cells in subsequent experiments. **(B)** Percentage of indels measured in all experimental and technical replicates using one gRNA for *SMAD2* and three for *SMAD3* in cells derived from two donors (donor 1 $n=4$, donor 2 $n=3$).

and Supplementary Fig. S4), supporting the result obtained for collagen deposition. Furthermore, in the double KO, we observed a decrease in collagen deposition, as well as a lack of expression of αSMA (Fig. 4B and C and Supplementary Fig. S4). These results differentiate the two SMAD proteins, demonstrating a critical role of SMAD3 in response to TGF-β stimulation for collagen production in contrast to SMAD2 in the Scar-in-a-Jar assay.

Discussion

Selection of disease-relevant targets is an important initial step in the drug discovery process. CRISPR technology enables perturbation of genes and pathways in human disease-relevant cellular systems as well as model organisms, enabling better understanding of the function and biology of a target.[19] However, the majority of published work utilizing gene editing is performed in less physiologically relevant immortalized cell lines because ge-

nome editing in primary cells presents numerous technical challenges. Here, we sought to optimize a gene editing workflow in patient-derived primary lung fibroblasts that enables studies of key mechanisms involved in lung fibrosis. We developed and extensively optimized a pipeline that uses easily accessible CRISPR-Cas9 RNP reagents and Nucleofector 4D electroporation, which results in >90% KO without the use of antibiotic selection or monoclonal expansion, reducing culture time. Moreover, our protocol allows the production of double gene KO cells, as demonstrated by the ablation of SMAD2 and SMAD3 proteins within the same sample. This result shows an important advancement of genome editing technology in primary cells, and we deliver a method that can be used to study the combinatorial effect of genes in a disease context.

Other groups have also reported genome editing in primary human cells, such as lung fibroblasts or bronchial epithelial cells,[20] airway epithelia,[21] and endothelial
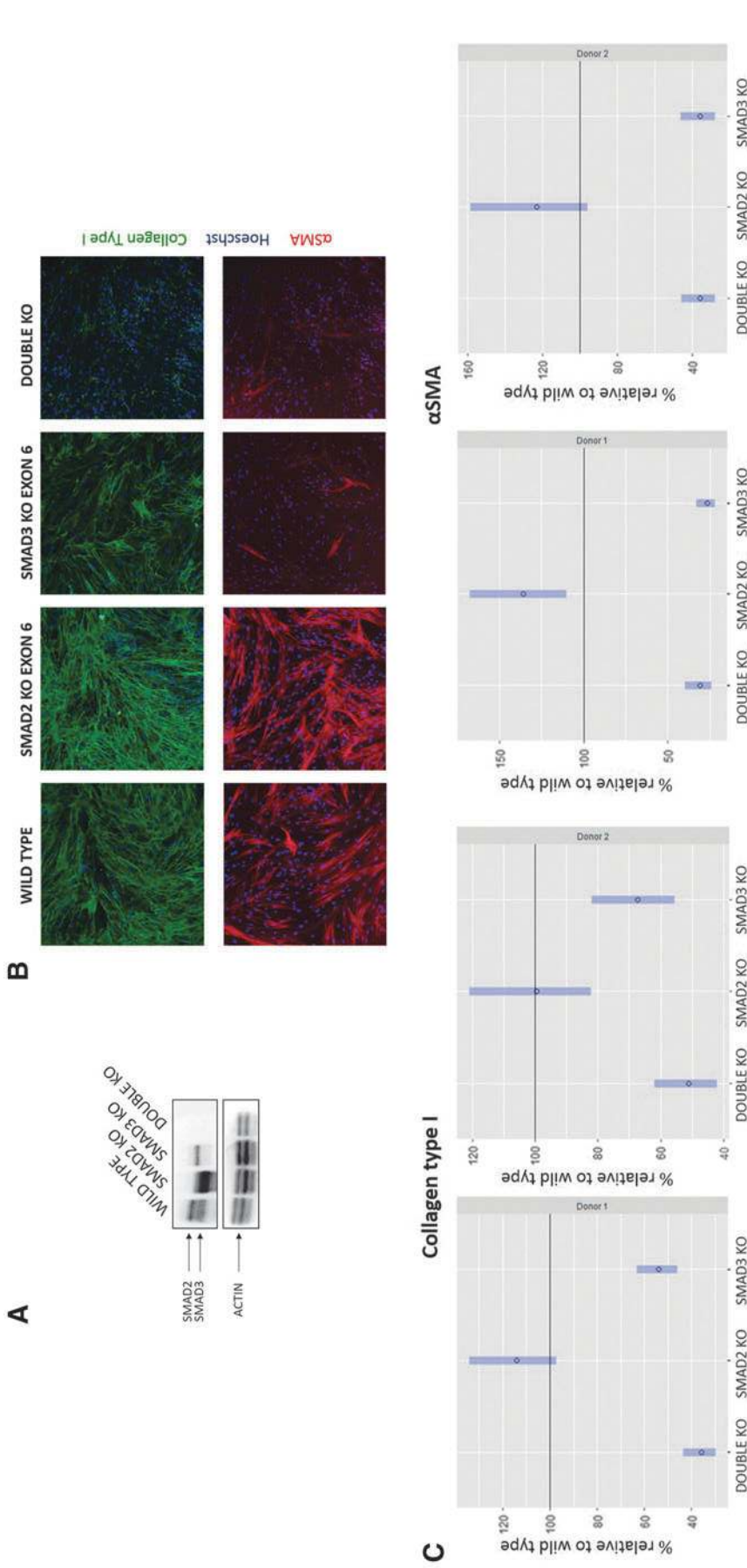
FIG. 4. Scar-in-a-Jar shows collagen deposition reduction in SMAD3 knockout (KO) and double KO cells. **(A)** Western blot analysis from wild type, SMAD2 KO, SMAD3 KO, and double SMAD2/SMAD3 KO cells. One antibody recognizing both SMAD proteins was used, as the two proteins share >90% homology of amino acid sequence. Actin was the loading control. Full-length Western blot is presented in Supplementary Figure S5. **(B)** Scar-in-a-Jar assay results. Collagen deposition was measured by immunofluorescence. Cells were also stained for Hoechst to visualize the nuclei and alpha smooth-muscle actin (αSMA) to detect the level of fibroblast differentiation. **(C)** Scar-in-a-Jar quantification of fluorescence estimated contrasts between KOs and wild-type TGF-β-stimulated cells across donors. The plots show the collagen type I and αSMA results (donor 1 $n = 3$, donor 2 $n = 2$). Dots are estimated differences; blue bars are 95% confidence intervals.

cells,[22] albeit at a reduced editing efficiency. These studies rely on the use of plasmid or viral CRISPR vectors (Supplementary Table S4 for technical comparison). CRISPR delivered as RNP complex has multiple advantages over these other formats, such as rapid editing within 3 h and fast clearance from cells by 24 h,[23] minimizing the possibility of off-target effects. Recently, highly efficient genome editing was achieved in primary human B cells,[24] human and mouse T cells,[25,26] as well as CD34+ hematopoietic stem and progenitor cells[26] by using RNP electroporation and a protocol similar to ours. Our workflow adds the important contribution of deep sequencing, which enables accurate editing efficiency measurement, regardless of cellular localization of the targeted proteins. Moreover, in our workflow, electroporation is performed using sample strips that process 16 different gRNAs simultaneously. Coupled with the deep sequencing genotyping, which measures hundreds of samples at the same time, we are able to increase the throughput of editing, enabling the generation of multiple gene KOs in one experiment. This can be critical in a context of target validation for a specific pathway or for a list of genes connected to a disease because it allows the function of many genes in the same experiment to be studied.

Optimization of editing conditions is required for every primary cell type used in an experiment. The process to identify optimum conditions used in this paper is relevant to any type of cell line or tissue. For example, we adapted this protocol to perform genome editing in primary CD4^{+} T cells (Supplementary Fig. S6). Achievement of near 100% editing efficiency will require identification of guides that cut with high efficiency and juxtaposition with optimum transfection conditions. To transfect primary fibroblasts, we found that electroporation with the 4D Nucleofector in the presence of an IDT electroporation enhancer gives the best results. We reproducibly achieved >90% editing efficiencies with >10 targets (data not shown). It is worth noting though that some primary cell types (e.g., T cells) do not tolerate inclusion of the electroporation enhancer. Furthermore, the optimization of electroporation in a new cell type needs to be tailored around different electroporation buffers, cell density, and examination of different gRNA:-Cas9 ratios.

Our workflow was developed to study targets for lung fibrosis. To demonstrate the value of our pipeline, we performed genome editing of SMAD2 and SMAD3 proteins, which function as transcriptional modulators activated by TGF-β. The signaling cascade activated by TGF-β triggers the phosphorylation of each protein that then form a complex with SMAD4. The SMAD proteins complexed together enter the nucleus and promote the transcription of pro-fibrotic genes.[27] However, it has been shown that they may be responsible for activation of different transcriptional programs.[27–29] In the context of disease, SMAD3, but not SMAD2, appears to be important for mediating TGF-β signaling in renal fibrosis,[30] hepatic fibrosis,[31] and cardiac fibrosis.[32] In contrast, SMAD2 is crucial for epiblast development and patterning of three germ layers during early developmental events.[28] Our data demonstrate that in the context of IPF, the presence of SMAD3 is critical for cell differentiation into myofibroblasts and collagen production in primary disease fibroblasts, as shown by the reduced amount of deposited collagen and lack of the myofibroblast differentiation marker αSMA in SMAD3 KO, but not SMAD2 KO. Moreover, in SMAD2 KO, we observed an increased expression of αSMA probably due to an enhanced activation of SMAD3, as already shown in hepatic and renal fibrosis.[30,31]

In this paper, we have tested the ability of cells to differentiate and produce collagen by performing a high-content cell imaging assay. Other phenotypic assays adopting transcriptomic analysis or measurement of secreted fibrosis mediators could also be deployed to examine what effect the perturbation of a target has in the context of lung fibroblast biology. It is worth noting that our workflow can be used to study the role of genes involved in several different pathologies in which fibroblasts from diverse organs contribute to tissue remodeling and could be used as a primary target validation tool for novel fibrosis targets. Moreover, the optimization processes we have described to enable efficient genome editing can be applied to other primary cell types and hence should facilitate genome editing in other contexts. In summary, we describe a novel pipeline to study gene function in the context of lung fibrosis that could also be useful for similar functional studies in other cell types.

Acknowledgments

Author Disclosure Statement

The authors declare no competing interests.

Supplementary Material

Supplementary Data
Supplementary Figure S1
Supplementary Figure S2
Supplementary Figure S3
Supplementary Figure S4

References

1. Klingberg F, Hinz B, White ES. The myofibroblast matrix: implications for tissue repair and fibrosis. *J Pathol* 2013;229:298–309. DOI: 10.1002/path.4104.
2. Perez EE, Wang J, Miller JC, et al. Establishment of HIV-1 resistance in CD4+ T cells by genome editing using zinc-finger nucleases. *Nat Biotechnol* 2008;26:808–816. DOI: 10.1038/nbt1410.
3. Kim HJ, Lee HJ, Kim H, et al. Targeted genome editing in human cells with zinc finger nucleases constructed via modular assembly. *Genome Res* 2009;19:1279–1288. DOI: 10.1101/gr.089417.108.
4. Brinkman EK, Chen T, Amendola M, et al. Easy quantitative assessment of genome editing by sequence trace decomposition. *Nucleic Acids Res* 2014;42:e168. DOI: 10.1093/nar/gku936.
5. Nelson CE, Hakim CH, Ousterout DG, et al. *In vivo* genome editing improves muscle function in a mouse model of Duchenne muscular dystrophy. *Science* 2016;351:403–407. DOI: 10.1126/science.aad5143.
6. Schmid-Burgk JL, Schmidt T, Gaidt MM, et al. OutKnocker: a web tool for rapid and simple genotyping of designer nuclease edited cell lines. *Genome Res* 2014;24:1719–1723. DOI: 10.1101/gr.176701.114.
7. Schmidt T, Schmid-Burgk JL, Ebert TS, et al. Designer nuclease-mediated generation of knockout THP1 cells. *Methods Mol Biol* 2016;1338:261–272. DOI: 10.1007/978-1-4939-2932-0_19.
8. Park J, Lim K, Kim JS, et al. Cas-analyzer: an online tool for assessing genome editing results using NGS data. *Bioinformatics* 2017;33:286–288. DOI: 10.1093/bioinformatics/btw561.
9. Pinello L, Canver MC, Hoban MD, et al. Analyzing CRISPR genome-editing experiments with CRISPResso. *Nat Biotechnol* 2016;34:695–697. DOI: 10.1038/nbt.3583.
10. Jacobi AM, Rettig GR, Turk R, et al. Simplified CRISPR tools for efficient genome editing and streamlined protocols for their delivery into mammalian cells and mouse zygotes. *Methods* 2017;121–122:16–28. DOI: 10.1016/j.ymeth.2017.03.021.
11. Keerthisingam CB, Jenkins RG, Harrison NK, et al. Cyclooxygenase-2 deficiency results in a loss of the anti-proliferative response to transforming growth factor-beta in human fibrotic lung fibroblasts and promotes bleomycin-induced pulmonary fibrosis in mice. *Am J Pathol* 2001;158:1411–1422.
12. Bates D, Mächler M, Bolker B, et al. Fitting linear mixed-effects models using lme4. *J Stat Softw* 2015;67. DOI: 10.18637/jss.v067.i01.
13. Matheson NJ, Peden AA, Lehner PJ. Antibody-free magnetic cell sorting of genetically modified primary human CD4+ T cells by one-step streptavidin affinity purification. *PLoS One* 2014;9:e111437. DOI: 10.1371/journal.pone.0111437.
14. Burr SP, Costa AS, Grice GL, et al. Mitochondrial protein lipoylation and the 2-oxoglutarate dehydrogenase complex controls HIF1alpha stability in aerobic conditions. *Cell Metab* 2016;24:740–752. DOI: 10.1016/j.cmet.2016.09.015.
15. Chen CZ, Peng YX, Wang ZB, et al. The Scar-in-a-Jar: studying potential antifibrotic compounds from the epigenetic to extracellular level in a single well. *Br J Pharmacol* 2009;158:1196–1209. DOI: 10.1111/j.1476-5381.2009.00387.x.
16. Mercer PF, Woodcock HV, Eley JD, et al. Exploration of a potent PI3 kinase/mTOR inhibitor as a novel anti-fibrotic agent in IPF. *Thorax* 2016;71:701–711. DOI: 10.1136/thoraxjnl-2015-207429.
17. Verrecchia F, Mauviel A. Transforming growth factor-beta signaling through the Smad pathway: role in extracellular matrix gene expression and regulation. *J Invest Dermatol* 2002;118:211–215. DOI: 10.1046/j.1523-1747.2002.01641.x.
18. Vaughan MB, Howard EW, Tomasek JJ. Transforming growth factor-beta1 promotes the morphological and functional differentiation of the myofibroblast. *Exp Cell Res* 2000;257:180–189. DOI: 10.1006/excr.2000.4869.
19. Lu Q, Livi GP, Modha S, et al. Applications of CRISPR genome editing technology in drug target identification and validation. *Expert Opin Drug Discov* 2017;12:541–552. DOI: 10.1080/17460441.2017.1317244.
20. Voets O, Tielen F, Elstak E, et al. Highly efficient gene inactivation by adenoviral CRISPR/Cas9 in human primary cells. *PLoS One* 2017;12:e0182974. DOI: 10.1371/journal.pone.0182974.
21. Chu HW, Rios C, Huang C, et al. CRISPR-Cas9-mediated gene knockout in primary human airway epithelial cells reveals a proinflammatory role for MUC18. *Gene Ther* 2015;22:822–829. DOI: 10.1038/gt.2015.53.
22. Gong H, Liu M, Klomp J, et al. Method for dual viral vector mediated CRISPR-Cas9 gene disruption in primary human endothelial cells. *Sci Rep* 2017;7:42127. DOI: 10.1038/srep42127.
23. DeWitt MA, Corn JE, Carroll D. Genome editing via delivery of Cas9 ribonucleoprotein. *Methods* 2017;121–122:9–15. DOI: 10.1016/j.ymeth.2017.04.003.
24. Johnson MJ, Laoharawee K, Lahr WS, et al. Engineering of primary human B cells with CRISPR/Cas9 targeted nuclease. *Sci Rep* 2018;8:12144. DOI: 10.1038/s41598-018-30358-0.
25. Seki A, Rutz S. Optimized RNP transfection for highly efficient CRISPR/Cas9-mediated gene knockout in primary T cells. *J Exp Med* 2018;215:985–997. DOI: 10.1084/jem.20171626.
26. Vakulskas CA, Dever DP, Rettig GR, et al. A high-fidelity Cas9 mutant delivered as a ribonucleoprotein complex enables efficient gene editing in human hematopoietic stem and progenitor cells. *Nat Med* 2018;24:1216–1224. DOI: 10.1038/s41591-018-0137-0.
27. Brown KA, Pietenpol JA, Moses HL. A tale of two proteins: differential roles and regulation of Smad2 and Smad3 in TGF-beta signaling. *J Cell Biochem* 2007;101:9–33. DOI: 10.1002/jcb.21255.
28. Liu L, Liu X, Ren X, et al. Smad2 and Smad3 have differential sensitivity in relaying TGFbeta signaling and inversely regulate early lineage specification. *Sci Rep* 2016;6:21602. DOI: 10.1038/srep21602.
29. Piek E, Ju WJ, Heyer J, et al. Functional characterization of transforming growth factor beta signaling in Smad2- and Smad3-deficient fibroblasts. *J Biol Chem* 2001;276:19945–19953. DOI: 10.1074/jbc.M102382200.
30. Meng XM, Huang XR, Chung AC, et al. Smad2 protects against TGF-beta/Smad3-mediated renal fibrosis. *J Am Soc Nephrol* 2010;21:1477–1487. DOI: 10.1681/ASN.2009121244.
31. Zhang L, Liu C, Meng XM, et al. Smad2 protects against TGF-beta1/Smad3-mediated collagen synthesis in human hepatic stellate cells during hepatic fibrosis. *Mol Cell Biochem* 2015;400:17–28. DOI: 10.1007/s11010-014-2258-1.
32. Khalil H, Kanisicak O, Prasad V, et al. Fibroblast-specific TGF-beta-Smad2/3 signaling underlies cardiac fibrosis. *J Clin Invest* 2017;127:3770–3783. DOI: 10.1172/JCI94753.